

Optimisation of microencapsulation of isophorone diisocyanate into polyurea shell by oil-in-water interfacial polymerisation

Liepa Pastarnokienė*,

Ernest Potapov,

Ričardas Makuška,

Tatjana Kochanė

*Department of Polymer Chemistry,
Vilnius University,
24 Naugarduko Street,
03225 Vilnius, Lithuania*

In this work, microcapsules containing isophorone diisocyanate (IPDI) encapsulated within a polyurea (PU) shell were synthesised via an oil-in-water emulsion interfacial polymerisation reaction involving tris(4-isocyanato phenyl)thiophosphate (TIPTP) and triethylenetetramine (TETA). Characterisation of the resulting microcapsules was conducted using Fourier transform infrared spectroscopy (FTIR), thermogravimetric analysis (TGA), optical microscopy and scanning electron microscopy (SEM). Various encapsulation parameters such as core-to-shell ratio, agitation speed, emulsifier type and concentration, and reaction time were systematically varied at four different levels. Optimisation of microencapsulation was performed using a Taguchi L16 parameter design approach, aiming to maximise desired outcomes (i.e. maximal core content and yield) while keeping the targeted microcapsule diameter of 50 µm. Under optimal conditions, the IPDI core content within microcapsules was up to 75% and the microcapsule yield was up to 49%.

Keywords: microencapsulation, isophorone diisocyanate, polyurea, interfacial polymerisation, Taguchi method

INTRODUCTION

Coatings are engineered with the primary objective of safeguarding the coated region against environmental and mechanical impairments, corrosion, and consequently extending the lifespan of the coated object significantly. Within the category of coatings, self-healing coatings exhibit a unique capability to autonomously repair mechanical damage or microcracks that may occur during their operational service. Numerous healing systems have undergone extensive testing over the years, with one such system involving the incorporation of microcapsules into the coating formulation [1–5]. These microcapsules contain healing agents such as epoxy resins [6–8], amines [9, 10], isocyanates [11–

15] and various kinds of oils [16–18]. If the coating is damaged, either through mechanical force or its inclination to shrink and crack, the microcapsules release healing agents into the affected area. This action forms a new barrier against the environment and seals the damaged area.

IPDI is a cycloaliphatic diisocyanate known for its two reactive isocyanate groups, which display distinct reactivity between primary and secondary NCO groups. This distinctive property imparts a high selectivity in reacting with hydroxyl-bearing compounds. It is commonly used in polyurethane foam formation [19–22] and polyurethane coatings [23–25]. IPDI is a great candidate for self-healing systems because of its low curing speed, low viscosity and good reactivity when mixed with alcohols, polyols, amines or water if catalysed [26–28].

* Corresponding author. Email: liepa.pastarnokiene@chgf.stud.vu.lt

The selection of shell materials holds significant importance as it can exert influence on both the core composition of the microcapsule and its integration into the coating system. Isocyanates can be encapsulated into several different shells like PU [29], polyurethane (PUR) [30], double walled – polyurea/melamine-formaldehyde (PU/MF) [31], polyurethane/urea-formaldehyde (PUR/UF) [32], or even biodegradable shell from polycaprolactone (PCL) [33]. In the referenced studies, microcapsules demonstrated variations in mechanical properties alongside differences in size, shell thickness, porosity and structure. Attaei et al. [29] described a synthesis technique for producing PU microcapsules using Desmodur RFE containing tris(p-isocyanatophenyl) thiophosphate (TIPTP) at 27 wt.% in ethyl acetate, IPDI and diethylenetriamine (DETA). PU microcapsules typically exhibited an average diameter of 10 μm with a shell thickness of 1.5 μm , presenting a smooth, nearly spherical morphology. Kardar et al. [30] investigated microcapsules with PUR shell material derived from various polyols. Morphological analysis revealed that the capsules synthesised using glycerol exhibited a wrinkled outer surface compared to those synthesised using 1,4-butanediol and 1,6-hexanediol. To enhance the mechanical properties of microcapsules, Du et al. [31] and Cruso et al. [32] developed microcapsules with a double shell. Double shell PU/MF microcapsules displayed elastomeric characteristics under small deformations (5.06%) and could recover after the applied force. However, under conditions of larger deformation (>14.53%), the microcapsules exhibited a viscoelastic behaviour and could not recover. In the case of PUR microcapsules coated with a second layer of UF, TGA indicated improved thermal stability compared to single-wall microcapsules.

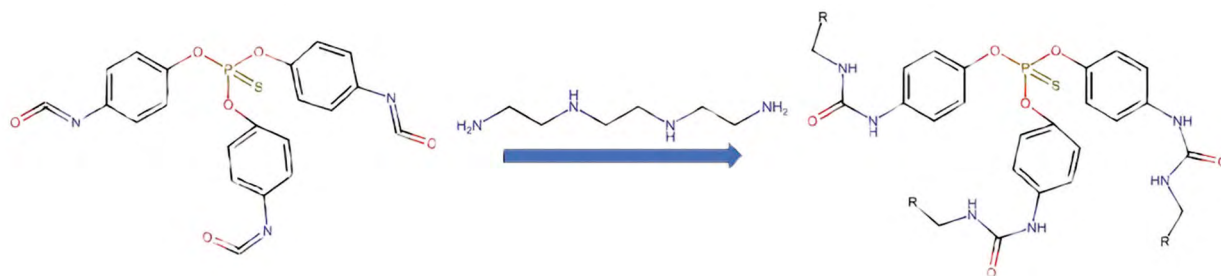
Several methods can be employed to create microcapsules for self-healing coatings including in situ polymerisation [34, 35], interfacial polymerisation [36–38], the solvent evaporation method [33, 39] and spray drying [40, 41]. In situ polymerisation and interfacial polymerisation are methods most commonly used in production of self-healing coating microcapsules from UF, MF, PU, PUR and others mainly due to the high active ingredient loading, moderately fast reaction, high yield and controllable synthesis process [42]. In comparison, the solvent evaporation technique usually tends to have lower active ingredient loading, lower yield, and thicker microcapsule shell formation [39, 42], although it can form more durable and more chemically resistant shells made from PCL [33] or with better interfacial interaction made from poly(methyl methacrylate) (PMMA) [18].

The purpose of the present study was to improve the process of microencapsulation of IPDI by interfacial polymerisation into a PU shell reaching a very high IPDI core content (Scheme 1). Another objective was optimisation of the microencapsulation process using the Taguchi's L16 parameter design approach enabling to find optimal parameters ensuring the maximal core content and, at the same, the formation of microcapsules with a size of 50 μm .

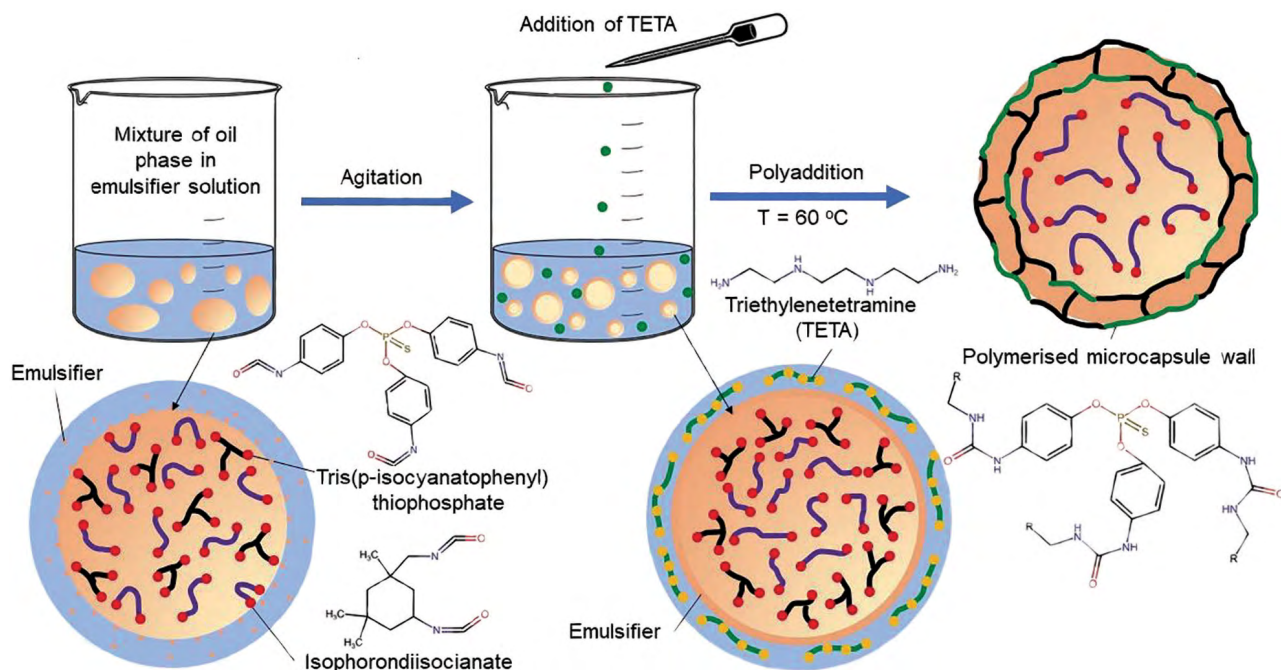
EXPERIMENTAL

MATERIAL AND METHODS

Isophorone diisocyanate (IPDI, NCO content 37.5%) and polyisocyanate under commercial name Desmodur RFE (27% solution of tris(4-isocyanatophenyl)thiophosphate (TIPTP) in ethyl acetate, NCO content of 7.2%) were supplied by Covestro AG. Triethylenetetramine (TETA)



Scheme 1. Chemical reaction between TIPTP and TETA that leads to formation of PU microcapsule shells



Scheme 2. Schematic representation of IPDI encapsulation into PU shell

was supplied by Huntsman. Sodium dodecylbenzenesulfonate (SDBS) was acquired from Eurochemicals. Gum Arabic (GA) was purchased from Thermo Fisher Scientific, while polyvinyl alcohol (PVA, deacetylation degree 85%) was obtained from Sigma-Aldrich.

Encapsulation of IPDI into PU shell

An example of the encapsulation of IPDI into a PU shell (experiment No. IE1)

The solution of the emulsifiers PVA 2%/GA 3% was prepared by dissolving PVA (3 g) and GA (4.5 g) in deionized water (142.5 g) and stirring overnight. The oil phase was prepared by mixing IPDI (13.3 g) with the solution of Desmodur RFE (15.6 g). The oil phase (28.9 g) was then added to the emulsifier solution (150 g) and stirred at 3000 rpm for 5 min. The resulting emulsion was set to stir at the constant speed of 1000 rpm while the temperature was increased up to 60°C. When the temperature reached the intended value, TETA was slowly added to the emulsion, and the emulsion was stirred at 1000 rpm for 30 min. To remove unreacted materials, the obtained microcapsules were washed with deionized water 4–5 times. Finally, the microcapsules were separated by freeze-drying at –55°C and 0.2 mbar.

Characterisation of microcapsules

The assessment of average microcapsule size, size distribution, and stability was conducted using an optical microscope Nikon Eclipse LV100ND. Further characterisation of microcapsule size, morphology and rupture was performed utilising a scanning electron microscope (SEM) Hitachi TM3000. The analysis of the microcapsules using FT-IR spectra within a range of 550–4000 cm^{-1} was carried out by a Jasco FT-IR 4600 spectrometer. The determination of the isophorone diisocyanate (IPDI) content within the microcapsules was executed through thermogravimetric analysis (TGA) using a Hitachi STA200 instrument. The TGA involved a heating rate of 40°C/min until reaching 150°C, followed by 10°C/min until 550°C, all under a nitrogen gas flow.

Design of experiment by Taguchi method

In the preliminary investigation it was identified that four pivotal parameters have the biggest potential to influence the core content, size of microcapsules and microcapsule yield. These parameters are the core-to-shell ratio, agitation speed, type and quantity of emulsifier, and reaction time. The chosen parameters and their respective levels are given in Table 1, with the range of levels determined through preliminary experimental assessments.

Table 1. Taguchi design parameters and their selected levels

Parameter, units	Levels			
	1	2	3	4
Core-to-shell ratio	2:1	3:1	4:1	5:1
Agitation speed, rpm	3000	4000	5000	6000
Emulsifier and its concentration, %	PVA 2/GA 3	PVA 1/GA 1.5	SDBS 1	GA 7
Reaction time, min	30	45	60	90

In this study, the Taguchi design methodology was employed to find the optimal process parameters using signal-to-noise ratio (SNR) analysis [43, 44]. The larger-the-better criterion (Eq. 1) was applied to discern the optimal conditions for attaining the maximum core content of the microcapsules and the highest reaction yield. Simultaneously, the nominal-the-best criterion (Eq. 2) was utilised to identify conditions conducive to the production of microcapsules with a size of 50 μm :

$$\frac{S}{N} = -10 \cdot \log \left(\frac{1}{n} \sum \frac{1}{y^2} \right) \quad \frac{S}{N} = -10 \cdot \log \frac{\bar{y}^2}{s^2}.$$

Larger-the-better

Nominal-the-best

In the equations, y represents the measured value of the core content (%) or the microcapsule

average size (μm), n is the number of measurements in a trial, and s is the nominal value.

RESULTS AND DISCUSSION

Encapsulation of IPDI into PU shell

The encapsulation process was studied using the L16 Taguchi method matrix, where 4 chosen parameters were changed throughout the synthesis. Three different signals were received and measured – the content of the healing agent IPDI inside microcapsules (core content), the microcapsule size and the microcapsule yield. Synthesis parameters and the signals are given in Table 2.

It was determined that some microcapsules tend to agglomerate more than others. During freeze-drying, which proceeds under deep vacuum, some microcapsules with thin or defectively formed shells were deformed and even ruptured.

Table 2. Data of microencapsulation of IPDI into PU shell

No.	Core: shell	Agitation speed, rpm	Emulsifier and its concentration, %	Reaction time, min	Core content, %	Microcapsule size range, μm	Average microcapsule size, μm	Microcapsule yield, %
IE1	2:1	3000	PVA 2/GA 3	30	58.9	20–90	35	36.7
IE2	3:1	4000	PVA 1/GA 1.5	45	64.1	20–90	45	58.9
IE3	4:1	5000	SDBS 1	60	72.3	10–40	20	74.3
IE4	5:1	6000	GA 7	90	78.6	20–90	60	26.9
IE5	2:1	4000	SDBS 1	90	52.2	10–20	10	84.3
IE6	3:1	5000	GA 7	30	61.7	15–110	60	56.0
IE7	4:1	6000	PVA 2/GA 3	45	74.6	8–20	15	25.2
IE8	5:1	3000	PVA 1/GA 1.5	60	76.1	30–120	80	32.6
IE9	2:1	5000	PVA 2/GA 3	60	58.3	10–40	35	6.5
IE10	3:1	6000	PVA 1/GA 1.5	90	65.8	20–60	40	12.6
IE11	4:1	3000	SDBS 1	30	66.4	10–60	25	6.0
IE12	5:1	4000	GA 7	45	69.7	30–60	50	29.4
IE13	2:1	6000	SDBS 1	45	49.9	10.0–20	10	71.5
IE14	3:1	3000	GA 7	60	74.6	20–70	50	48.9
IE15	4:1	4000	PVA 2/GA 3	90	71.8	20–70	40	16.8
IE16	5:1	5000	PVA 1/GA 1.5	30	73.1	20–80	40	19.3

After the rupture, the core content of the microcapsules was released and spread among other microcapsules which invoked sticking them together and agglomerating. Agglomeration can also be caused by an unsuitable emulsifier chosen for the system. It was determined that the microcapsules obtained in the presence of SDBS as an emulsifier had higher tendency to agglomerate than those obtained using GA or PVA/GA solutions (Table 3). Moreover, using 1% SDBS as an emulsifier led to the smallest microcapsule size. It is known that small particles have a higher tendency to agglomeration which leads to formation of much larger aggregates [45].

Characterisation of the prepared microcapsules

The prepared microcapsules were analysed using optical microscopy and scanning electron microscopy to evaluate the microcapsule size, size distribution, stability in an aqueous solution and in a dry state, and resistance to rupture under applied force (Figs 1, 2).

It was determined by optical microscopy that the microcapsules synthesised in the presence of 1% SDBS as emulsifier were agglomerated both in water and when dried. The agglomerates measured 300–1000 μm in size were made up from 10–60 μm microcapsules stuck together and remained

agglomerated even after washing and freeze-drying. In contrast, the microcapsules synthesised using GA and GA/PVA as emulsifiers were stable, round and dispersed evenly. When pressed between two glass panels, the microcapsules underwent collapse, and the subsequently released healing agent was observed between the glass panels. This observation signifies a high efficiency in the encapsulation of the healing agent and suggests the presence of thin microcapsule walls that can be easily damaged.

Scanning electron microscopy (SEM) was used to measure the microcapsule size as well as visualise their surface and form, and determine the approximate thickness of microcapsule shell (Fig. 2). Before the experiment, some microcapsules were crushed using a metal spatula to examine the rupture picture and microcapsule shell thickness. As it is seen from the SEM images, the microcapsule surface is smooth with slight indentations which could be caused by freeze-drying process. It was determined that the microcapsule shell was very thin, with the thickness of about 1–3 μm , that is why it can be easily crushed.

Microcapsules IE8 were added to polyaspartic acid ester/isocyanate through the coating which was cured. The clear coating was examined with an optical microscope trying to determine

Table 3. Stability of the synthesised microcapsules

No.	Emulsifier/concentration, %	Stability in solution	Stability after drying	Microcapsule size range, μm	Average microcapsule size, μm
IE1	PVA 2/GA 3	Stable	Stable	20–90	35
IE2	PVA 1/GA 1.5	Stable	Stable	20–90	45
IE3	SDBS 1	Agglomerated	Agglomerated	10–40	20
IE4	GA 7	Stable	Stable	20–90	60
IE5	SDBS 1	Agglomerated	Agglomerated	10–20	10
IE6	GA 7	Stable	Stable	15–110	60
IE7	PVA 2/GA 3	Stable	Stable	8–20	15
IE8	PVA 1/GA 1.5	Stable	Stable	30–120	80
IE9	PVA 2/GA 3	Stable	Stable	10–40	35
IE10	PVA 1/GA 1.5	Stable	Stable	20–60	40
IE11	SDBS 1	Agglomerated	Agglomerated	10–60	25
IE12	GA 7	Stable	Stable	30–60	50
IE13	SDBS 1	Agglomerated	Agglomerated	10–20	10
IE14	GA 7	Stable	Stable	20–70	50
IE15	PVA 2/GA 3	Stable	Stable	20–70	40
IE16	PVA 1/GA 1.5	Stable	Agglomerated	20–80	40

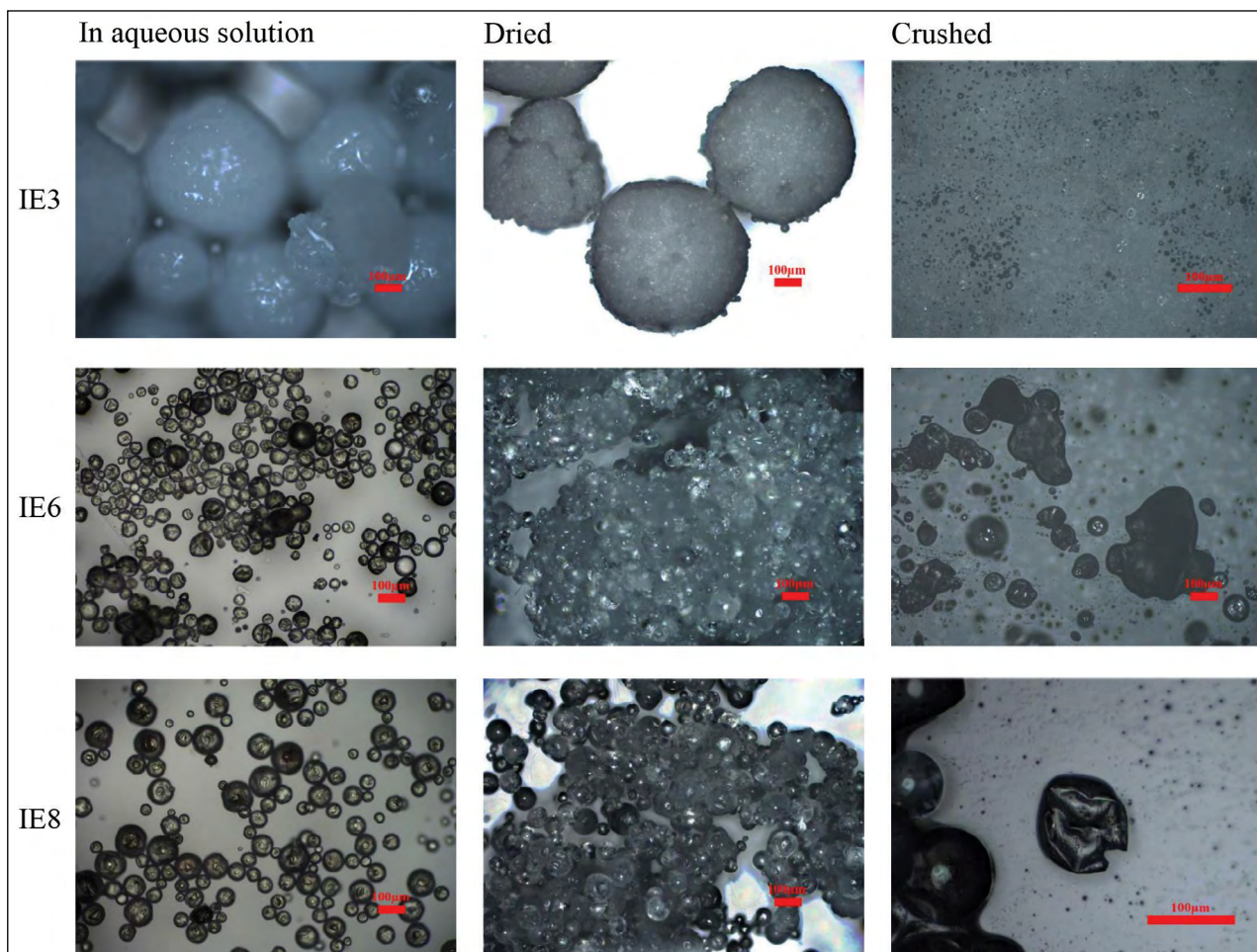


Fig. 1. Optical microscope images of the microcapsules IE3, IE6 and IE8

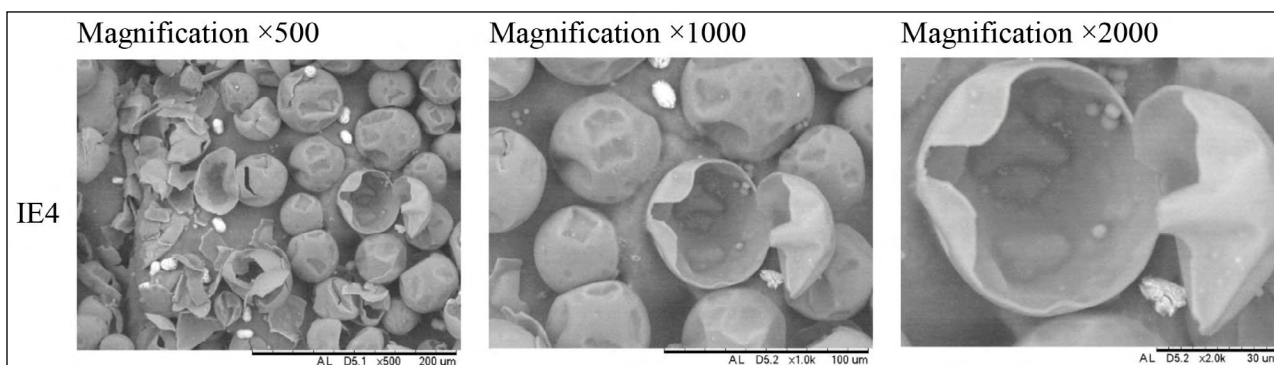


Fig. 2. SEM images of the crushed microcapsules IE4

microcapsule dispersibility inside the coating as well as microcapsule ability to rupture when a crack appears (Fig. 3).

The microcapsules inside the cured coating were dispersed evenly and did not agglomerate or rupture. The crosscut of coating showed that microcapsules were conjugated with the coating and split in two parts when the coating was broken.

A part of the healing agent is seen near the rupture place as oil splatter (Fig. 3).

FTIR spectra of IPDI (core material), RFE+TETA (cured shell material) and microcapsules IE14 were recorded and presented in Fig. 4. The absorption band of the stretching vibrations of N–H at about 3350 cm^{-1} and the absorption bands of C=O and N–H in the carbamide group

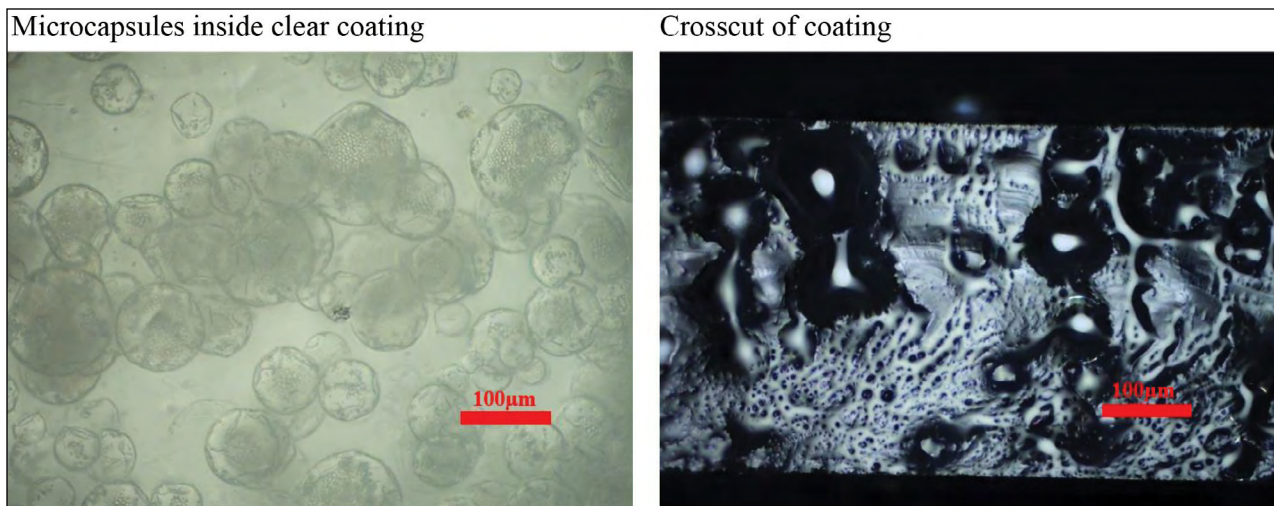


Fig. 3. Optical microscope images of microcapsules IE8 inside a clear coating and a coating crosscut

at about 1510 and 1650 cm^{-1} , respectively, are characteristic of PU shell material and are seen in the spectra of the shell material and microcapsule. An intensive absorption band of the stretching vibrations of $\text{N}=\text{C}=\text{O}$ in isocyanate groups appears at about 2250 cm^{-1} in both spectra of IPDI and

microcapsules IE14; this proves that the encapsulation of IPDI as core material was successful.

For the determination of core content in microcapsules, the thermogravimetric analysis (TGA) of the core material and microcapsules was done (Fig. 5). IPDI evaporation and destruction

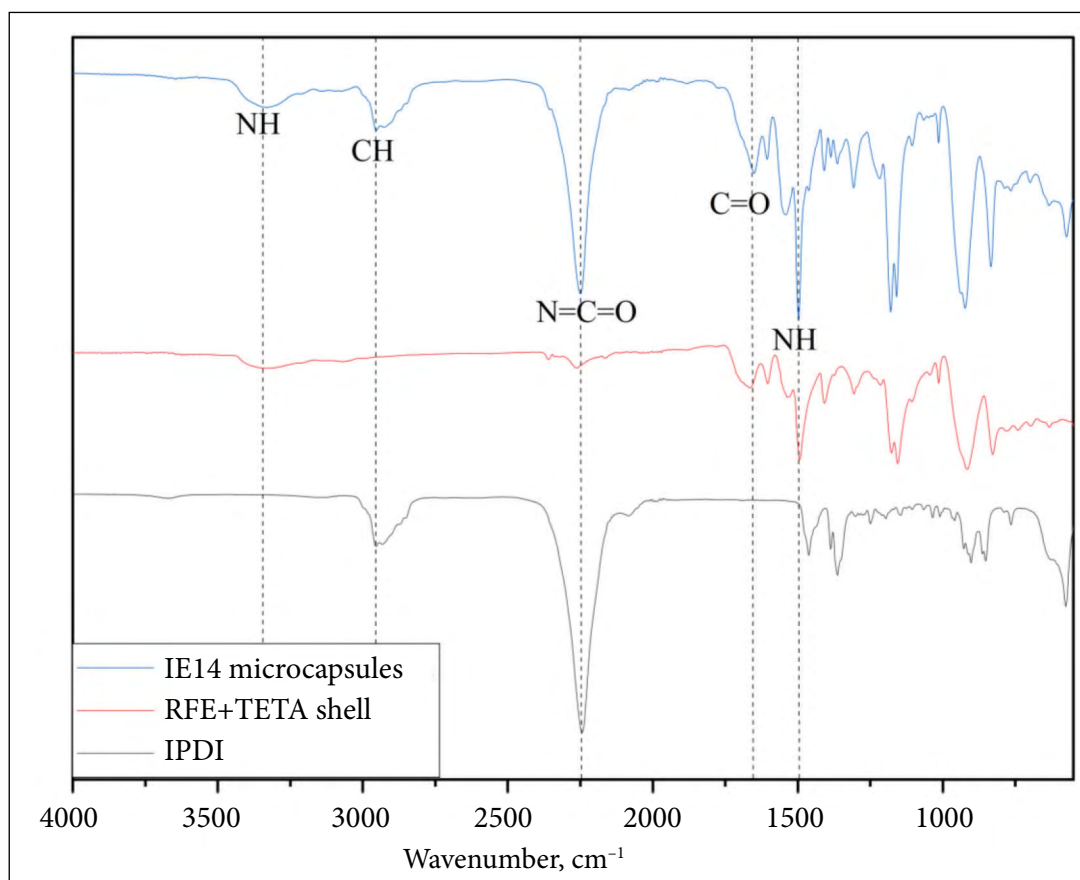


Fig. 4. FTIR spectra of IPDI as core material, RFE+TETA as microcapsule shell, and microcapsules IE14

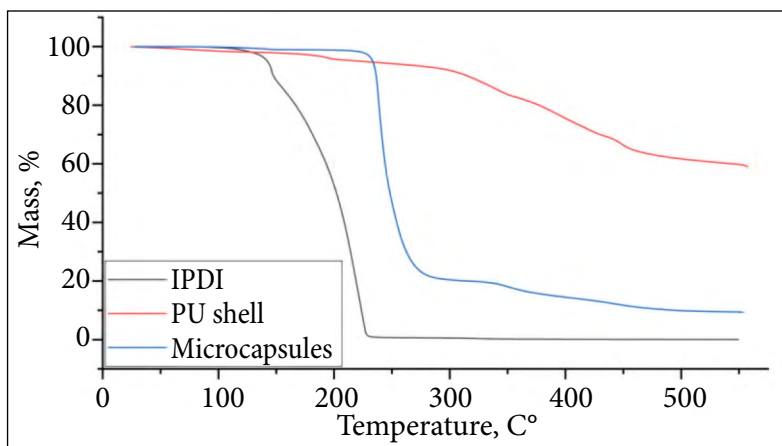


Fig. 5. TGA curves of the core material IPDI, shell material PU and microcapsules IE4

start at about 130°C and continues until approx. 240°C. The first stage of degradation of the shell material PU starts at about 150°C and lasts until 200°C; this part of degradation could be attributed to the destruction of unreacted shell material TETA, TIPTP and the evaporation of ethyl acetate. The actual destruction of PU starts at about 250°C and lasts until 550°C and even further. The microcapsule IE 4 analysis demonstrates that 79% of the microcapsule materials are destroyed at temperatures below 300°C. This part of the weight loss could be contributed to IPDI. Slightly higher destruction temperature of IPDI in microcapsules is expected since IPDI is entrapped inside a PU shell, and destruction can only begin when the shell is damaged by rising pressure inside the microcapsule or under degradation. The core content of the microcapsules was in a range of 50 to 79%.

Optimisation of the encapsulation process

The Taguchi method was employed in this study to identify the optimal parameters to achieve the highest core content, a microcapsule size closest to 50 µm, and the maximum microcapsule yield. Four distinct synthesis parameters, namely the core-to-shell ratio, agitation speed, emulsifier type and concentration, and reaction time, were systematically varied throughout the experimental process. The signal-to-noise ratio (SNR) was calculated using the larger-the-better criterion to discern optimal conditions for the core content and yield, while the nominal-the-best criterion was applied for the optimisation of microcapsule size. The results are summarised in Fig. 6.

The highest SNR value and significantly higher core content (Fig. 6a) were achieved using the core-to-shell ratio 5:1. The agitation speed had a small impact to the core content, but the best results were at the agitation speed 3000 rpm. Three emulsifiers – PVA 1%/GA 1.5%, PVA 2%/GA 3% and GA 7% – had a similar impact on the core content with a small superiority of GA 7%; anionic emulsifier SDBS was not suitable in achieving a high core content. The reaction time also had a rather small impact to the core content, although the highest core content was at the reaction time 60 min. Considering four key parameters, the core-to-shell ratio and the choice of emulsifiers had the highest impact on the microcapsule core content (Fig. 7).

The optimal microcapsule size closest to 50 µm (Fig. 6b) was achieved at various combinations of the reaction parameters. Considering the core-to-shell ratio, the optimal microcapsule size was at the ratio 3:1 and 5:1; at the ratio 2:1 and 4:1, the microcapsules tended to be either too large or too small. The agitation speed had lower impact on the microcapsule size while the optimal microcapsule size was at the agitation speed 4000 rpm. The emulsifier had a strong impact on the microcapsule size. Microcapsules of the optimal size were preferentially formed in the presence of GA 7% as an emulsifier. SDBS was not suitable as an emulsifier since it promoted agglomeration of the microcapsules. The reaction time had a minimal impact on the microcapsule size, but the optimal time was 45 min. Considering the four reaction parameters, the choice of emulsifiers and the core-to-shell ratio had the highest impact on the microcapsule size (Fig. 6).

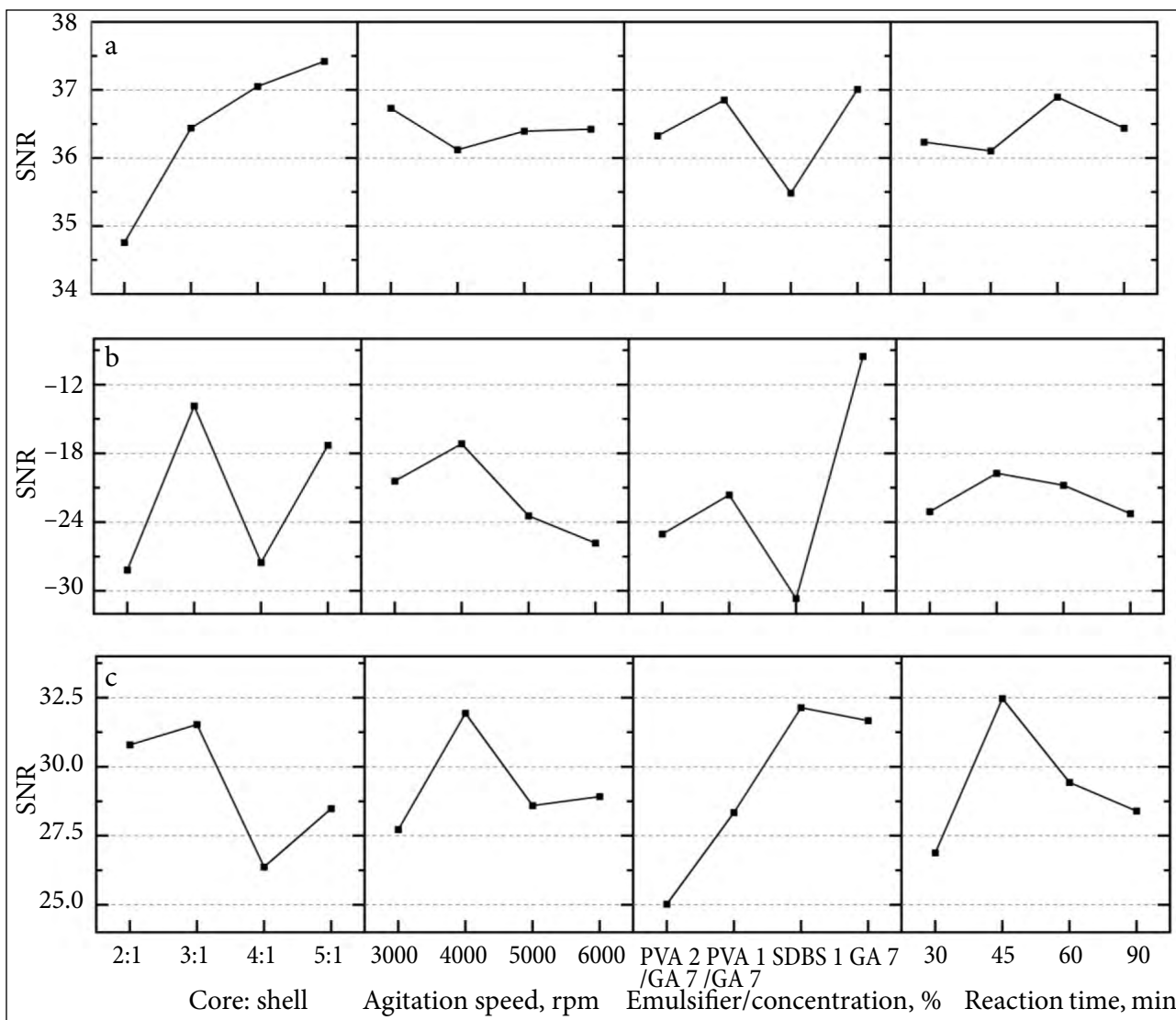


Fig. 6. SNR plots according to the Taguchi method; the dependence of the microcapsule core content (a), microcapsule size (b) and microcapsule yield (c) on the microencapsulation parameters: core-to-shell ratio, agitation speed, type and concentration of emulsifier, and reaction time

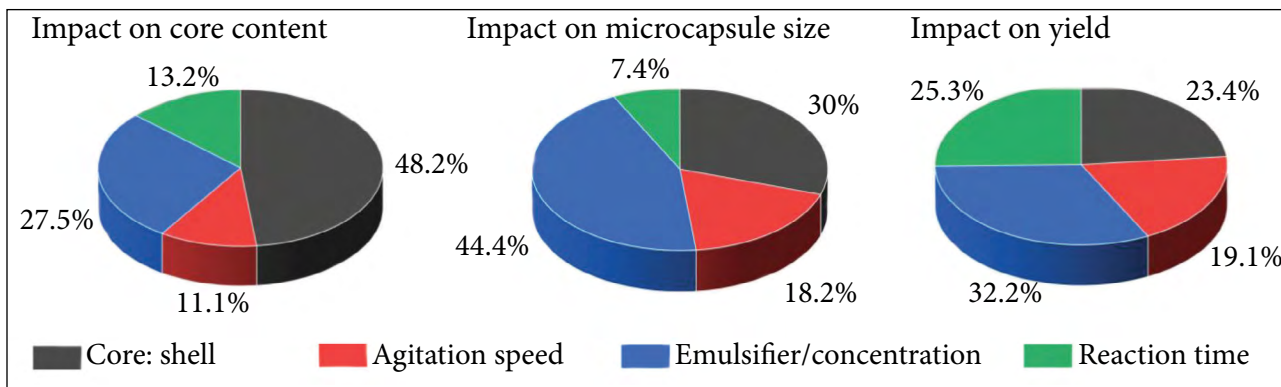


Fig. 7. Impact of the reaction parameters on the microcapsule core content, size and yield

The highest yield of microcapsules (Fig. 6c) was obtained at the core-to-shell ratio 3:1; the ratio 4:1 was the most unfavourable. The optimal agita-

tion speed regarding yield was 4000 rpm. The optimal emulsifier promoting the highest yield of microcapsules was SDBS 1%. Possibly, this could

be explained by agglomeration of microcapsules in the presence of SDBS, since losses of large agglomerates during washing and drying processes are minimal. The highest yield was achieved at the reaction time 45 min. The impact of the four parameters on the yield of microcapsules was similar (Fig. 7), moreover, the yield is very much dependent on the time given for the microcapsules to settle before they are separated from liquid after washing. Optimal conditions for the microencapsulation of IPDI in the PU shell regarding the highest core content, optimal microcapsule size of 50 μm and the highest yield include the core-to-shell ratio 3:1, the agitation speed 3000 rpm, Gum Arabic (7%) as an emulsifier and the reaction time 60 min.

CONCLUSIONS

Microencapsulation of IPDI into a PU shell was done by oil-in-water emulsion interfacial polymerisation. The microencapsulation process was optimised using the Taguchi L16 parameter design with four chosen parameters – core-to-shell ratio, agitation speed, emulsifier/concentration and reaction time – and three signals – core content, microcapsule size and reaction yield. Optimal conditions for the microencapsulation of IPDI into the PU shell regarding the highest core content, optimal microcapsule size of 50 μm and the highest yield include the core-to-shell ratio 3:1, the agitation speed 3000 rpm, Gum Arabic (7%) as an emulsifier and the reaction time 60 min. Under optimal conditions, the IPDI core content within the microcapsules was up to 75% and the microcapsule yield was up to 49%. The Taguchi's experimental design enabled the efficient optimisation of the IPDI microencapsulation process with a reduced number of experiments. The synthesised IPDI microcapsules could potentially be used in self-healing coatings, whether in single or double capsule systems.

Received 5 July 2024
Accepted 30 August 2024

References

1. Y. Zhao, W. Zhang, L. Liao, S. Wang, W. Li, *Appl. Surf. Sci.*, **258**(6), 1915 (2012).

2. X. Liu, H. Zhang, J. Wang, Z. Wang, S. Wang, *Surf. Coat. Tech.*, **206**(23), 4976 (2012).
3. C. Zhang, H. Wang, Q. Zhou, *Prog. Org. Coat.*, **125**, 403 (2018).
4. D. Sun, H. Zhang, X. Tang, J. Yang, *Polymer*, **91**, 33 (2016).
5. T. Siva, S. Sathiyarayanan, *Prog. Org. Coat.*, **82**, 57 (2015).
6. Y. Jialan, Y. Chenpeng, Z. Chengfei, H. Baoqing, *Prog. Org. Coat*, **132**, 440 (2019).
7. F. Safaei, S. N. Khorasani, H. Rahnama, R. E. Neisiany, M. S. Koochaki, *Prog. Org. Coat*, **114**, 40 (2018).
8. S. Parsaee, S. M. Mirabedini, R. Farnood, F. Alizadegan, *J. Appl. Polym. Sci.*, **137**(41), 49663 (2020).
9. H. Yi, Y. Deng, C. Wang, *Compos. Sci. Technol.*, **133**, 51 (2016).
10. H. Jin, C. L. Mangun, D. S. Stradley, J. S. Moore, N. R. Sottos, S. R. White, *Polymer*, **53**(2), 581 (2012).
11. D. Sun, Y. B. Chong, K. Chen, J. Yang, *Chem. Eng. J.*, **346**, 289 (2018).
12. H. Li, X. Wang, *Polymer*, **262**, 125478 (2022).
13. E. Koh, N. Kim, J. Shin, Y. Kim, *RSC Adv.*, **4**(31), 16214 (2014).
14. M. Huang, J. Yang, *J. Mater. Chem.*, **21**(30), 11123 (2011).
15. S. V. Karpov, V. P. Lodygina, V. V. Komratova, A. S. Dzhalumukhanova, G. V. Malkov, E. R. Badamshina, *Kinet. Catal.*, **57**(4), 422 (2016).
16. S. Lang, Q. Zhou, *Prog. Org. Coat*, **105**, 99 (2017).
17. J. Li, H. Shi, F. Liu, E. Han, *Prog. Org. Coat*, **156**, 106236 (2021).
18. A. H. Navarchian, N. Najafipoor, F. Ahangaran, *Prog. Org. Coat*, **132**, 288 (2019).
19. H. Choe, J. H. Kim, *J. Ind. Eng. Chem.*, **69**, 153 (2018).
20. S. M. Hasan, J. E. Raymond, T. S. Wilson, B. K. Keller, D. J. Maitland, *Macromol. Chem. Phys.*, **215**(24), 2420 (2014).
21. R. Heath, *R. Brydson's Plastics Materials*, 799 (2017).
22. M. Ates, S. Karadag, A. A. Eker, B. Eker, *Polym. Int.*, **71**(10), 1157 (2022).
23. V. V. Gite, P. P. Mahulikar, D. G. Hundiwale, *Prog. Org. Coat*, **68**(4), 307 (2010).
24. E. Spyrou, H. Metternich, R. Franke, *Prog. Org. Coat*, **48**(2), 201 (2003).
25. C. Yu, M. Salzano de Luna, A. Russo, et al., *Adv. Mater. Interfaces*, **8**(10), 2100117 (2021).
26. Y. Wei, X. Jiang, S. Li, X. Z. Kong, *Eur. Polym. J.*, **115**, 384 (2019).
27. M. Guo, W. Li, N. Han, et al., *Polymers*, **10**(3), 319 (2018).
28. S. V. Karpov, V. P. Lodygina, V. V. Komratova, A. S. Dzhalumukhanova, G. V. Malkov, E. R. Badamshina, *Kinet. Catal.*, **57**(3), 319 (2016).
29. M. Attaei, L. M. Calado, M. G. Taryba, et al., *Prog. Org. Coat*, **139**, 105445 (2019).

30. P. Kardar, *Prog. Org. Coat*, **89**, 271 (2015).
31. G. Du, J. Hu, J. Zhou, et al., *Chin. J. Chem. Eng.*, **28(5)**, 1459 (2020).
32. M. M. Caruso, B. J. Blaiszik, H. Jin, et al., *ACS Appl. Mater. Interfaces*, **2(4)**, 1195 (2010).
33. M. V. Loureiro, M. Vale, R. Galhano, S. Matos, J. C. Bordado, I. Pinho, A. C. Marques, *ACS Appl. Polym. Mater.* **2(11)**, 4425 (2020).
34. E. Katouezadeh, S. M. Zebarjad, K. Janghorban, *J. Mater. Res. Technol.*, **8(1)**, 541 (2018).
35. H. Zhang, W. Li, R. Huang, N. Wang, J. Wang, X. Zhang, *New J. Chem.*, **41(23)**, 14696 (2017).
36. X. Ji, J. Li, W. Hua, Y. Hu, B. Si, B. Chen, *Constr. Build. Mater.*, **289**, 123179 (2021).
37. F. Yu, Y. Wang, Y. Zhao, J. Chou, X. Li, *Materials*, **14(13)**, 3753 (2021).
38. F. Ricardo, D. Pradilla, R. Luiz, O. A. Solano, *Polymers*, **13(4)**, 644 (2021).
39. J. Fan, Y. Zheng, Y. Xie, et al., *Compos. Sci. Technol.*, **138**, 80 (2017).
40. E. Assadpour, S. M. Jafari, *Annu. Rev. Food Sci. Technol.*, **10(1)**, 103 (2019).
41. S. Shamaei, S. S. Seiedlou, M. Aghbashlo, E. Tsotsas, A. Kharaghani, *Innov. Food Sci. Emerg. Technol.*, **39**, 101 (2017).
42. D. Y. Zhu, M. Z. Rong, M. Q. Zhang, *Prog. Polym. Sci.*, **49–50**, 175 (2015).
43. Ç. Özada, M. Ünal, E. K. Şahin, H. Özer, A. R. Motorcu, M. Yazıcı, *Multidiscip. Model. Mater. Struct.*, **18(6)**, 1049 (2022).
44. A. N. Mustapha, Y. Zhang, Z. Zhang, Y. Ding, Q. Yuan, Y. Li, *J. Mater. Res. Technol.*, **11**, 667 (2021).
45. T. Ogholaja, D. O. Njobuenwu, M. Fairweather, *Proceedings of ESCAPE-27*, 79 (2017).

Liepa Pastarnokienė, Ernest Potapov, Ričardas Makuška, Tatjana Kochanė

IZOFORONO DIIZOCIANATO ĮKAPSULIAVIMO Į POLIKARBAMIDO APVALKALĄ, NAUDOJANT TARPFAZINĘ POLIMERIZACIJĄ, OPTIMIZAVIMAS

S an t r a u k a

Mikrokapsulės, sudarytos iš įkapsuliuoto izoforono diizocianato (IPDI) ir polikarbamido (PU) apvalkalo, buvo gautos tarpfazinės polimerizacijos metodu kaip reagentus naudojant tris(4-izocianatofenil)tiofosfatą (TIPTP) ir trietilentetraminą (TETA). Mikrokapsulės buvo apibūdintos naudojant FTIR spektroskopiją, termogravimetrinę analizę (TGA), optinę mikroskopiją ir skenuojančią elektroninę mikroskopiją (SEM). Vykdam mikrokapsuliavimą buvo sistemingai keturiais lygiais keičiami didžiausią įtaką procesui turintys parametrai, tokie kaip įkapsuliuojamos medžiagos ir apvalkalo santykis, maišymo greitis, emulsiklio tipas ir koncentracija bei reakcijos trukmė. Siekiant gauti maksimalų rezultatą – didžiausią santykinę įkapsuliuotos medžiagos dalį mikrokapsulėse ir didžiausią mikrokapsulių išeigą, išlaikant tikslinį 50 µm mikrokapsulių skersmenį, – mikrokapsuliavimo procesas buvo optimizuotas naudojant Taguchi metodą L16 parametų. Mikrokapsuliavimą vykdant optimaliomis sąlygomis, IPDI kiekis mikrokapsulėse siekė 75 %, o mikrokapsulių išeiga – 49 %.